2011 International Symposium on Nonlinear Theory and its Applications
NOLTA2011, Kobe, Japan, September 4-7, 2011

Origin of the quasi-periodic solutions with three-phase synchronized envelope in a ring of three-coupled bistable oscillators

Kyohei Kamiyama†, Motomasa Komuro‡ and Tetsuro Endo†

†Department of Electronics and Bioinfomatics, Meiji University
1-1-1 Higashi-Mita, Tama-ku, Kawasaki-shi, Kanagawa, 214-8571 Japan
‡Department of Occupational Therapy, Teikyo University of Science
2525 Yatsusawa, Uenohara-shi, Yamanashi, 409-0193 Japan
Email: kamiyama@meiji.ac.jp, komuro@ntu.ac.jp, endoh@isc.meiji.ac.jp

Abstract— In this paper, we try to find the origin of quasi-periodic propagating wave solutions with three-phase synchronized envelope in a ring of three-coupled bistable oscillators. We obtain two-parameter bifurcation diagram in relation to coupling factor versus nonlinear strength starting from the quasi-periodic solution, and we find several Arnold tongues showing the synchroized regions with various periods. By investigating the bifurcation on the boundary of these Arnold tongues, we clarify the appearance and disappearance mechanisms of the quasi-periodic solution.

1. Introduction

Research on pulse wave propagation phenomena in coupled oscillator systems is important from theoretical as well as practical point of view in relation to information transmission using active transmission line represented by SOLITON [1, 2, 3, 4, 5]. The authors performed computer simulation of pulse wave propagation phenomena in a large number of coupled bistable oscillator systems [2] and bifurcation analysis from standing pulse wave to propagating pulse wave in a ring consisting of comparatively small number of bistable oscillators (6 units) [3]. As a result, it is clarified that various bifurcations including pitchfork, saddle-node, and heteroclinic bifurcations are related to the transition from standing pulse wave to the propagating pulse wave [6]. However, even a six-coupled oscillator system was still high dimensional (12 dimensional), and therefore, detailed theoretical analysis was difficult. Therefore, we investigate simpler system; namely, a ring of three-coupled bistable oscillators (6 dimensional), and clarify the bifurcation mechanism from standing to propagating pulse wave or its inverse. In particular, bifurcation mechanisms of the quasi-periodic solutions with three-phase synchronized envelope which is introduced in [7], is elucidated. How the transition from the standing periodic wave solution to the propagating quasi-periodic wave solution occurs is investigated, and as a result, we notice that it is due to the combination of pitchfork bifurcation of the periodic solution and heteroclinic bifurcation of the quasi-periodic solution similar to [3].

2. Circuit and Equation

Our circuit model is shown in Fig. 1(a) in which three bistable oscillators are coupled through inductor(L_0). Each oscillator model is shown in Fig. 1(b) which has nonlinear conductor(NC) whose V-I characteristic is written by : $i_{NC} = g_1 v - g_3 v^3 + g_5 v^5 for g_1, g_3, g_5 > 0$. Circuit equation is written by Eq. (1) where α is a coupling strength, β is a control parameter of amplitude and ϵ presents a parameter showing nonlinear strength. *Throughout the paper,* β *and* ϵ *are set as* $\beta = 3.20$ *and* $\epsilon = 0.50$.

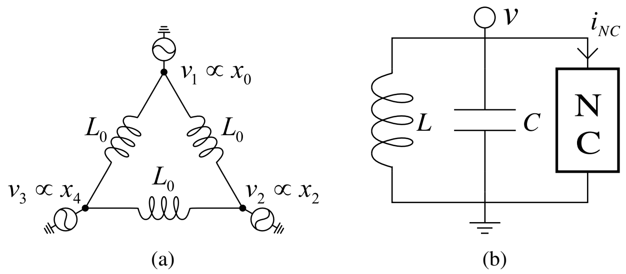

Fig. 1. Circuit model. (a) Ring of three-coupled bistable oscillators. (b) Bistable oscillator. V-I characteristic is written by : $i_{NC} = g_1 v - g_3 v^3 + g_5 v^5$ for $g_1, g_3, g_5 > 0$.

$$
\begin{aligned}
\dot{x}_0 &= x_1 \\
\dot{x}_1 &= -\epsilon(1 - \beta x_0^2 + x_0^4)x_1 \\
&\quad - (1-\alpha)x_0 + \alpha(x_4 - 2x_0 + x_2) \\
\dot{x}_2 &= x_3 \\
\dot{x}_3 &= -\epsilon(1 - \beta x_2^2 + x_2^4)x_3 \\
&\quad - (1-\alpha)x_2 + \alpha(x_0 - 2x_2 + x_4) \\
\dot{x}_4 &= x_5 \\
\dot{x}_5 &= -\epsilon(1 - \beta x_4^2 + x_4^4)x_5 \\
&\quad - (1-\alpha)x_4 + \alpha(x_2 - 2x_4 + x_0)
\end{aligned} \tag{1}
$$

3. Bifurcation related to the quasi-periodic solution $ICC3\phi$

In Fig. 1 we can obtain a quasi-periodic solution as shown in Fig. 2 for a certain parameter set. This is propagating wave solution rotating around the ring of Fig. 1(a)

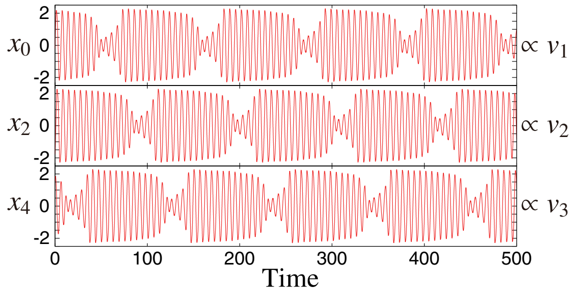

Fig. 2. *ICC*3ϕ propagating to the right direction. Variables x_0, x_2, and x_4 are proportional to v_1, v_2, and v_3, respectively. Parameter is set as follows: $\alpha = 0.08$. Initial condition is given by $x_2(0) = 2, x_4(0) = 1, x_5(0) = 1$ and others = 0

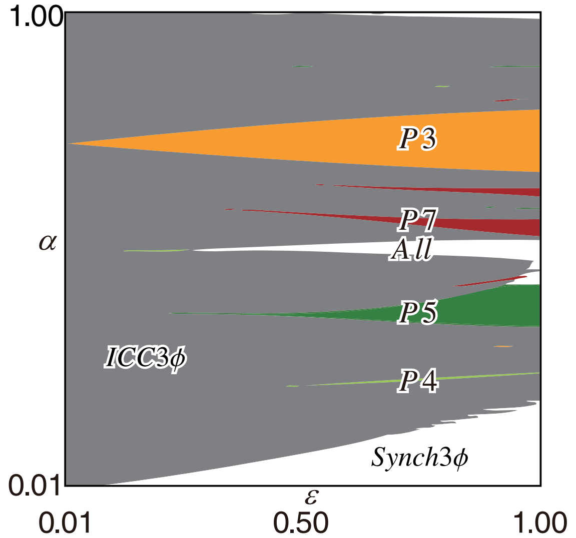

Fig. 3. Two-parameter bifurcation diagram of *ICC*3ϕ in relation to ϵ and α obtained by brute force computer simulation using continuation method. P_k denotes k-periodic solution.

in the right direction [1]. In particular, the envelopes of each oscillation x_0, x_2 and x_4 are synchronized with three-phase. This is the same type of quasi-periodic solution as that introduced in [7]. For some parameter sets the quasi-periodic solution becomes periodic due to phase-locking of the component frequencies. We call these quasi-periodic or periodic solutions *ICC*3ϕ generically. Further, we call the former one the "unlocked *ICC*3ϕ" and the latter one the "locked *ICC*3ϕ". Figure 3 is a two parameter bifurcation diagram of *ICC*3ϕ in relation to ϵ and α [2]. There are many Arnold tongues representing the region of locked solutions such as $P3, P4, P5, P7$, etc. We notice the important fact

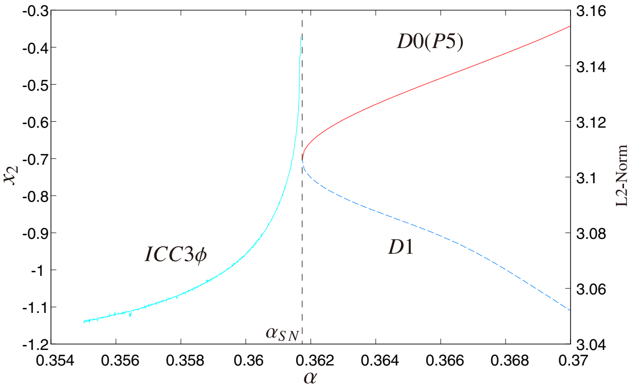

Fig. 4. One-parameter bifurcation diagram of the locked and unlocked $P5$ *ICC*3ϕ in terms of α. The $D0$ denotes the locked solution and *ICC*3ϕ denotes the unlocked solution shown by L2-norm. D_k denotes a fixed point with k-dimensional instability.

from further investigation that the boundary curves of $P3$ present pitchfork bifurcation and some hysteresis exists in the transition between unlocked and locked *ICC*3ϕ which is investigated later. While, those for other periodic solutions present saddle-node bifurcation and no hysteresis exists between unlocked and locked regions. In the region "*All*", the same phase synchronized solution appears, and in the region "*Synch*3ϕ", synchronized three-phase solution does. In these regions *ICC*3ϕ vanishes.

4. Transition between locked and unlocked *ICC*3ϕ for the $P5$ Arnold tongue (SN bifurcation)

At first, we will investigate the transition between locked and unlocked *ICC*3ϕ for the $P5$ Arnold tongue. The same bifurcation can be observed in other Arnold tongues except $P3$. Figure 4 presents a one-parameter bifurcation diagrams in terms of α. Note that unlocked *ICC*3ϕ starts with the SN bifurcation point of the locked *ICC*3ϕ. This means that the transition between the locked and unlocked *ICC*3ϕ has no hysteresis. Figure 5 demonstrates (a) time waveform in the locked case, (b) Poincare map of the attractors in the unlocked (closed curve) and locked (circle points) cases, (c) the associated DFT Poincare maps. Note that the three circle points are on the invariant closed curve which means there is no "discontinuity" in the transition between locked and unlocked *ICC*3ϕ.

5. Transition between locked and unlocked *ICC*3ϕ for the $P3$ Arnold tongue (PF bifurcation)

In this section we will investigate bifurcation on the boundary of $P3$ Arnold tongue. Figure 6 presents a one-parameter bifurcation diagram of the locked *ICC*3ϕ denoted by $D0$ and unlocked *ICC*3ϕ. These two curves overlap to some extent which means there is a certain amount of hysteresis between the transition. The periodic solu-

[1] There exists the same solution rotating in the left direction for different initial condition.

[2] Figure 3 is obtained as follows. Realize *ICC*3ϕ by choosing $(\epsilon, \alpha) = (0.1, 0.1)$ for $x_1(0) = -2.0, x_2(0) = 2.0$, others are zero. Then judge locked or unlocked *ICC*3ϕ by increasing ϵ with constant α by using continuation method.

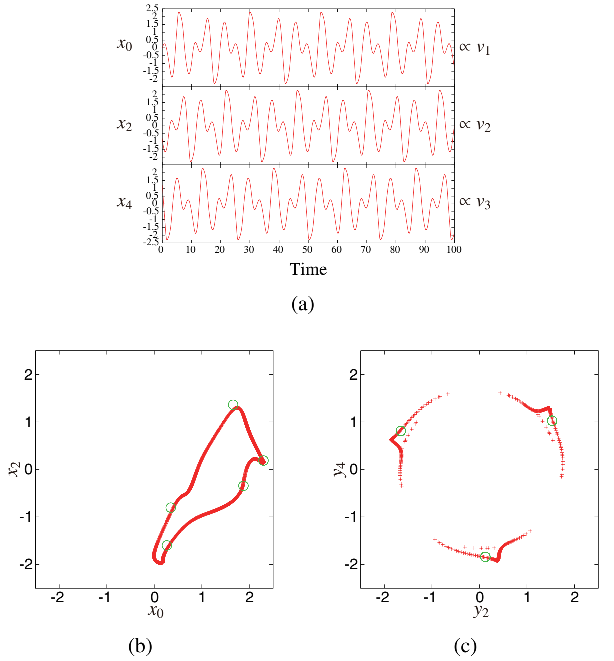

Fig. 5. Attractors around the SN bifurcation point of the $P5$ Arnold tongue. (a) Time waveform inside the tongue ($\alpha = 0.37$). (b) Invariant curve showing unlocked solution ($\alpha = 0.36$) and points showing locked solution ($\alpha = 0.37$) on the Poincare section ($x_1 = 0$, plus to minus). (c) Those on the DFT Poincare map.

tion loses its stability by pitchfork bifurcation, and the quasi-periodic solution does by heteroclinic bifurcation. Figure 7 demonstrates (a) time waveform in locked case, (b) Poincare map of the attractors in the unlocked (closed curve) and locked (circle points) cases, (c) the associated DFT Poincare maps. The circle points representing the locked $ICC3\phi$ are not on the invariant closed curve representing the locked $ICC3\phi$ which means that there is some discontinuity between the transition. In particular, there is only one circle point on the DFT Poincare map which is different from the former case in Fig. 5(c). This is because that in the $P3$ locked solution rotational symmetry is no more maintained as seen in Fig. 7(a). While, in the $P5$ locked solution rotational symmetry is kept as seen in Fig. 5(a). Figure 8 presents schematic diagrams showing the variation of the unstable manifold (UM) of $\tilde{D}1, \tilde{D}1'$ and $D1$ of Fig. 6 in terms of α. Defining α_{c1} and α_{c2} are the values of heteroclinic tangency [3], behavior of the UM is classified in four cases. For $\alpha_{c2} < \alpha$, $D0$, periodic solution $P3$ is the only stable solution. For $\alpha_{c1} < \alpha < \alpha_{c2}$ heteroclinic tangle occurs. The $D0$ is the only stable solution. One of the UMs starting from $\tilde{D}1$ and $\tilde{D}1'$ behaves chaotically. For $\alpha_{PF} < \alpha < \alpha_{c1}$ $D0$ and $ICC3\phi$ coexist. For $\alpha < \alpha_{PF}$ only $ICC3\phi$ exists. Figure 9 demonstrates the actual UM associated with Fig. 8(c) (upper half). Figure 10 demonstrates an example of the heteroclinic bifurcation. For $\alpha < \alpha_{c1}$, UM goes to $D0$. For $\alpha_{c1} < \alpha < \alpha_{c2}$, UM is stretched in two directions, which is one of the evidences of heteroclinic tangency. For $\alpha_{c2} < \alpha$, UM goes to $ICC3\phi$.

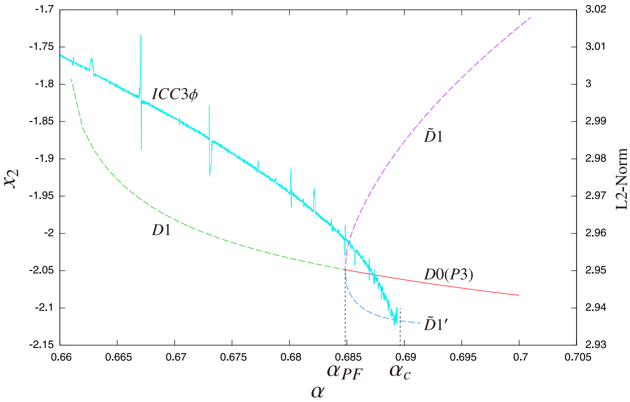

Fig. 6. One-parameter bifurcation diagram of the locked and unlocked $P3$ $ICC3\phi$ in terms of α. The $D0$ denotes the locked solution and $ICC3\phi$ denotes the unlocked solution shown by L2-norm.

6. Conclusion

We elucidate bifurcation mechanism of the transition between the locked $ICC3\phi$ and the unlocked $ICC3\phi$ in a ring of three-coupled bistable oscillators. Here, $ICC3\phi$ is a quasi-periodic propagating wave solution in general whose envelope is synchronized in three phase. We already know that in a ring of six-coupled bistable oscillators, the standing wave (periodic) solution in which only one oscillator is alive and others are all death, can bifurcate to the corresponding propagating (quasi-periodic) wave solution. Therefore, at first, we investigate the bifurcation of the standing wave solution in which one oscillator is alive and others are death with the increase of coupling factor. But, we cannot obtain the corresponding propagating wave solution, even if coupling factor is increased. Therefore, we focus our attention to the transition between locked and unlocked $ICC3\phi$. As a result, we find that the transition from $P3$ $ICC3\phi$ (periodic solution) to unlocked $ICC3\phi$ (quasi-peiodic solution) is due to pitchfork bifurcation, and the inverse bifurcation is due to heteroclinic bifurcation. This transition includes some amount of hysteresis. In addition, we find that the transition between the locked $ICC3\phi$ other than $P3$ and unlocked one is due to saddle-node bifurcation, and the transition includes no hysteresis. As a future problem, we will investigate other bifurcations of $ICC3\phi$.

References

[1] Y. Nishiura, D. Ueyama, and T. Yanagita, "Chaotic pulses for discrete reaction diffusion systems," SIAM Journal on

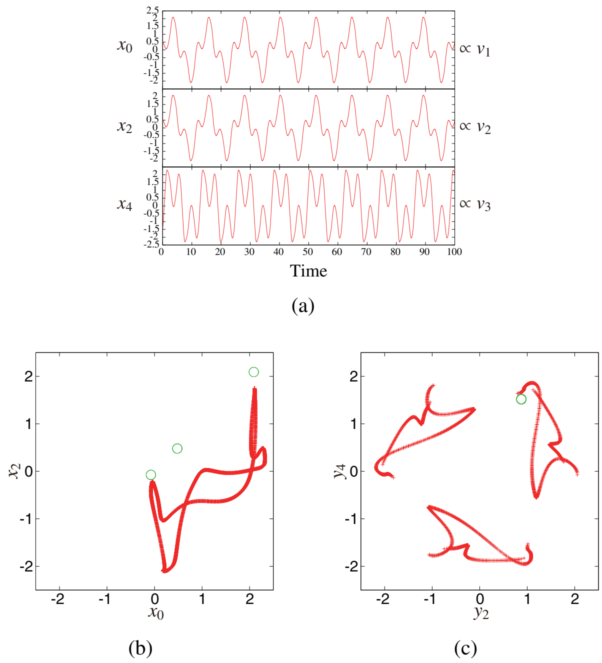

Fig. 7. Attractors around the PF bifurcation point of the $P3$ Arnold tongue. (a) Time waveform inside the tongue ($\alpha = 0.69$). (b) Invariant curve showing unlocked solution ($\alpha = 0.68$) and points showing locked solution ($\alpha = 0.69$) on the Poincare section ($x_1 = 0$, plus to minus). (c) Those on the DFT Poincare map.

Applied Dynamical Systems, vol.4, no.3, pp.733–754, Aug. 2006.

[2] K. Shimizu, T. Endo, and D. Ueyama, "Pulse wave propagation in a large number of coupled bistable oscillators," IEICE Trans. Fundamentals, vol.E91-A, no.9, pp.2540–2545, Sept. 2008.

[3] K. Shimizu, M. Komuro, and T. Endo, "Onset of the propagating pulse wave in a ring of coupled bistable oscillators," NOLTA, IEICE, vol.2, no.1, pp.139–151, Jan. 2011.

[4] M. Yamauchi, Y. Nishino, A. Ushida, and M. Tanaka, "Phase-inversion waves in oscillators coupled by two kinds of inductors as a ladder," IEICE Trans. Fundamentals, vol.E87-A, no.9, pp.2233–2240, Sept. 2004.

[5] J.P. Keener, "Propagation and its failure in coupled systems of discrete excitable cells," SIAM Journal on Applied Mathematics, vol.47, no.3, pp.556–572, June 1987.

[6] K. Kamiyama, M. Komuro, T. Endo, and K. Shimizu, "Propagating pulse wave observed in a ring of six-coupled hard-type van der pol oscillators — a case starting from type 2 standing wave —," IEICE Tech. Rep., vol.110, no.465, pp.69–76, March 2011.

[7] T. Yoshinaga and H. Kawakami, "Synchronized quasi-periodic oscillations in a ring of coupled oscillators with hard characteristics," IEICE Trans. A, vol.75, no.12, pp.1811–1818, Dec. 1992.

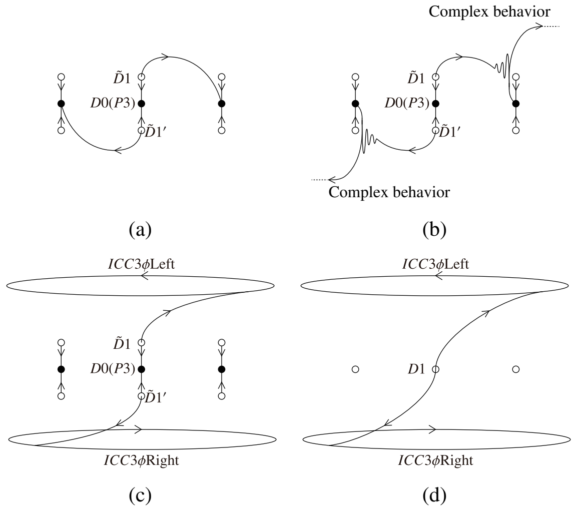

Fig. 8. Schematic diagrams showing qualitative change of unstable manifolds according to the values of α. (a) $\alpha_{c2} < \alpha$. (b) $\alpha_{c1} < \alpha < \alpha_{c2}$. (c) $\alpha_{pf} < \alpha < \alpha_{c1}$. (d) $\alpha < \alpha_{pf}$. The UM's starting from one of three $D0$'s only are drawn to avoid jamming.

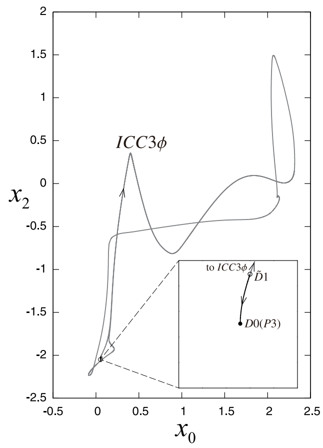

Fig. 9. Actual behavior of $ICC3\phi$ for Fig. 8(c) for $\alpha = 0.6852$. Upper half is drawn.

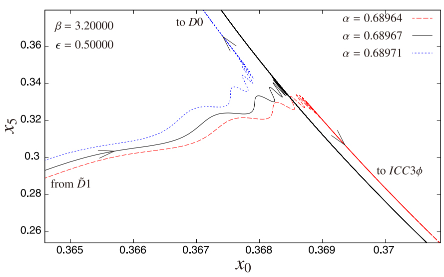

Fig. 10. Heteroclinic behavior of the UM starting from the $\tilde{D}1$ saddle. For $\alpha = 0.68964 < \alpha_{c1}$ the UM goes to $D0$. For $\alpha = 0.68967$ it is stretched in two directions. For $\alpha = 0.68971 > \alpha_{c2}$ it goes to $ICC3\phi$.